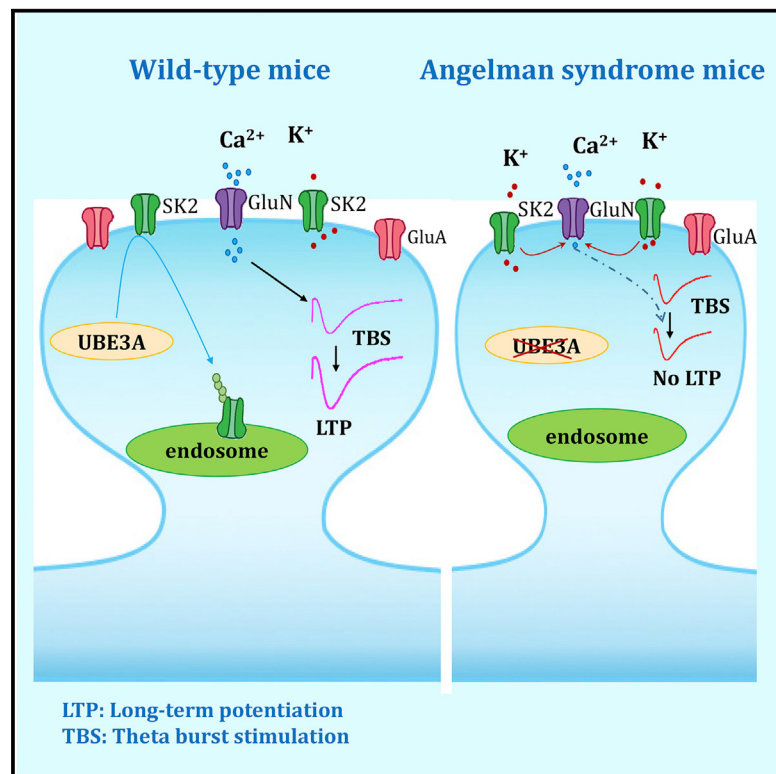


# UBE3A Regulates Synaptic Plasticity and Learning and Memory by Controlling SK2 Channel Endocytosis

## Graphical Abstract



## Authors

Jiandong Sun, Guoqi Zhu, Yan Liu, ..., Yun Luo, Michel Baudry, Xiaoning Bi

## Correspondence

xbi@westernu.edu

## In Brief

Sun et al. show that UBE3A, an ubiquitin E3 ligase whose deficiency results in Angelman syndrome, regulates synaptic plasticity and learning and memory by directly modulating synaptic levels of the small-conductance potassium channels, SK2 channels. They demonstrate that UBE3A ubiquitinates SK2 channels, resulting in their removal from synapses.

## Highlights

- UBE3A deficiency is associated with increased levels of synaptic SK2 channels
- UBE3A ubiquitinates SK2 channels in the C-terminal domain, resulting in endocytosis
- UBE3A-deficit-induced changes in LTP and LTD are reversed by SK2 channel blockade
- SK2 channel blockade improves hippocampal-dependent learning in UBE3A-deficient mice



# UBE3A Regulates Synaptic Plasticity and Learning and Memory by Controlling SK2 Channel Endocytosis

Jiandong Sun,<sup>1</sup> Guoqi Zhu,<sup>2</sup> Yan Liu,<sup>1</sup> Steve Standley,<sup>1</sup> Angela Ji,<sup>1</sup> Rashmi Tunuguntla,<sup>1</sup> Yubin Wang,<sup>1</sup> Chad Claus,<sup>1</sup> Yun Luo,<sup>1</sup> Michel Baudry,<sup>1</sup> and Xiaoning Bi<sup>1,\*</sup>

<sup>1</sup>Western University of Health Sciences, Pomona, CA 91766, USA

<sup>2</sup>Key Laboratory of Xin'an Medicine, Ministry of Education, Anhui University of Traditional Chinese Medicine, Hefei 230038, China

\*Correspondence: [xbi@westernu.edu](mailto:xbi@westernu.edu)

<http://dx.doi.org/10.1016/j.celrep.2015.06.023>

This is an open access article under the CC BY-NC-ND license (<http://creativecommons.org/licenses/by-nc-nd/4.0/>).

## SUMMARY

Gated solely by activity-induced changes in intracellular calcium, small-conductance potassium channels (SKs) are critical for a variety of functions in the CNS, from learning and memory to rhythmic activity and sleep. While there is a wealth of information on SK2 gating, kinetics, and  $\text{Ca}^{2+}$  sensitivity, little is known regarding the regulation of SK2 subcellular localization. We report here that synaptic SK2 levels are regulated by the E3 ubiquitin ligase UBE3A, whose deficiency results in Angelman syndrome and overexpression in increased risk of autistic spectrum disorder. UBE3A directly ubiquitinates SK2 in the C-terminal domain, which facilitates endocytosis. In UBE3A-deficient mice, increased postsynaptic SK2 levels result in decreased NMDA receptor activation, thereby impairing hippocampal long-term synaptic plasticity. Impairments in both synaptic plasticity and fear conditioning memory in UBE3A-deficient mice are significantly ameliorated by blocking SK2. These results elucidate a mechanism by which UBE3A directly influences cognitive function.

## INTRODUCTION

Information processing in CNS circuits depends on synaptic activity. In particular, synaptic transmission is modulated by different small-conductance calcium-activated potassium channels (SKs), which either contribute to the afterhyperpolarization that follows an action potential or facilitate repolarization following excitatory postsynaptic potentials (EPSPs). SKs participate in various CNS functions, from regulating neuronal intrinsic excitability to network rhythmic activity and higher brain functions (Adelman et al., 2012; Colgin et al., 2005; Ohtsuki et al., 2012). In hippocampal CA1 pyramidal neurons, synaptic SK2s are opened upon N-methyl-D-aspartate receptor (NMDAR) activation and repolarize the membrane, thereby terminating NMDAR function (Ngo-Anh et al., 2005). This local feedback loop between NMDARs and SK2s has been proposed to play a critical role in regulating neuronal excitability and in controlling

the threshold for induction of long-term potentiation (LTP) (Hammond et al., 2006; Lin et al., 2008). LTP induction also regulates synaptic SK2 expression, as it triggers endocytosis of synaptic SK2s (Lin et al., 2008).

Accumulating evidence indicates that a number of postsynaptic proteins are ubiquitinated in an activity-dependent manner (Colledge et al., 2003; Ehlers, 2003; Guo and Wang, 2007; Patrick et al., 2003). Ubiquitination consists of modifying proteins through E3-ligase-mediated ubiquitin attachment (Komander et al., 2009). One of the E3 ligases, UBE3A, is critical for normal brain function (Huibregtse et al., 1995), since its deficiency causes Angelman syndrome (AS) (Williams et al., 1990) whereas its overexpression is linked to an increased risk of autistic spectrum disorder (Cook et al., 1997). However, to date, very few neuronal substrates of UBE3A have been identified. The current study provides evidence that UBE3A directly ubiquitinates the C-terminal domain of SK2, thereby facilitating its internalization. Deficiency in this regulation accounts for impairments in LTP and learning and memory found in UBE3A-deficient mice.

## RESULTS

### Synaptic SK2 Levels Are Increased in Hippocampus of UBE3A-Deficient Mice

Previous research from several groups, including our own, has shown that LTP is impaired in maternal UBE3A-deficient (AS) mice (Baudry et al., 2012; Jiang et al., 1998; van Woerden et al., 2007). We hypothesized that UBE3A may directly regulate synaptic SK2 expression and that its deficiency could contribute to LTP impairment. Western blot analysis of proteins from different hippocampal subcellular fractions (Figures S1A and S1B) showed that SK2 levels were significantly higher in crude synaptosomal (P2; Figure 1A) and PSD-enriched (P3; Figure 1B) fractions of AS mice than in those from wild-type (WT) mice. SK2 levels in whole hippocampal homogenates were not significantly different between WT and AS mice (Figure S1C). Immunofluorescent staining showed that the highest levels of SK2 expression in the hippocampal CA1 region were in cell bodies and dendrites of pyramidal neurons (Figure 1C; Figure S1E). High-magnification examination revealed that SK2-immunoreactive puncta were distributed along apical dendrites and were partially co-localized with PSD95- (Figure 1C) and synaptophysin-immunopositive profiles (Figure S1E). Quantitative analysis showed that the

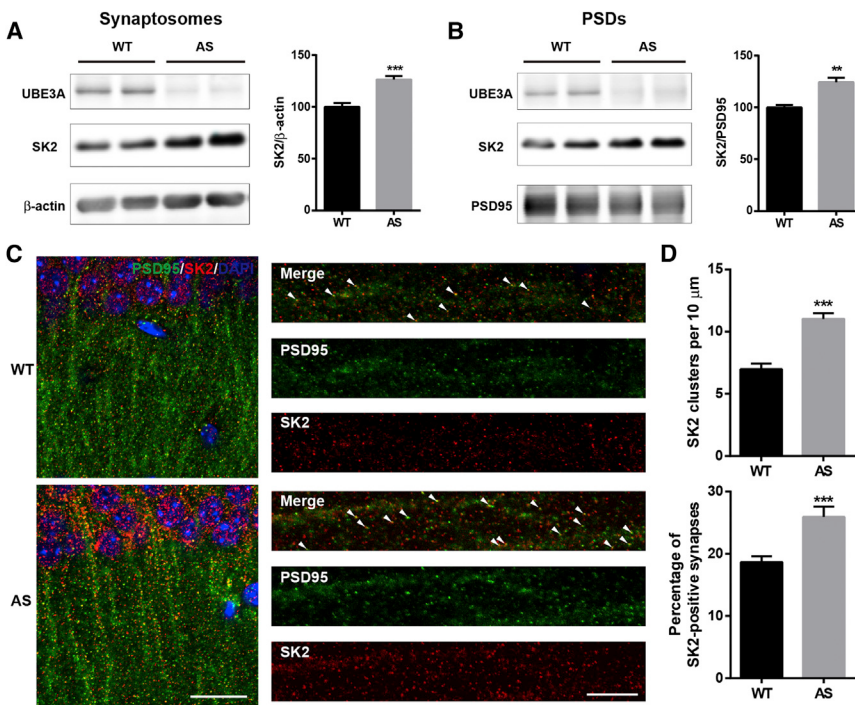


**Figure 1. SK2 Expression in Hippocampus of AS and WT Mice**

(A and B) Western blot analysis of SK2 levels in (A) crude synaptosomal fractions (P2) and (B) PSD fractions (P3). Optical densities of the SK2 band are normalized to those of β-actin or PSD-95. Data are expressed as % of values in WT mice and shown as means ± SEM of nine or ten (A) or three mice (B) from at least three litters; \*\*\*p < 0.001 (unpaired t test) and \*\*p < 0.01 (unpaired t test).

(C) Localization of synaptic SK2 in AS mice. Representative images of CA1 pyramidal neurons stained with anti-SK2 (red) and -PSD95 (green) antibodies. Arrowheads indicate clearly co-localized puncta. Scale bar represents 20 μm (left) or 10 μm (right).

(D) Quantitative analysis of the number of SK2-immunoreactive puncta and percentage of SK2 and PSD95 dually stained puncta/synapses in hippocampal CA1 region. Shown are means ± SEM; n = 18–24 regions of interest from at least nine slices from at least three mice per group (unpaired t test, \*\*\*p < 0.001).

See also Figure S1.

number of SK2-immunopositive puncta was markedly increased in AS mice (Figure 1D). The percentage of puncta dually stained with SK2 and PSD95 (Figure 1D) or SK2 and synaptophysin (Figure S1F) was also significantly increased in AS mice. There was no significant difference in the overall number of PSD95-immunopositive puncta between AS and WT mice (Figure S1D).

### Reduced SK2 Protein Ubiquitination in Hippocampus of AS Mice

Next, we determined whether the increase in synaptic SK2 levels in AS mice was due to the lack of UBE3A-mediated ubiquitination. Immunofluorescent staining showed that UBE3A and SK2 were co-localized in puncta along apical dendrites of CA1 pyramidal neurons (Figure 2A) and dendrites of cultured hippocampal neurons from WT mice (Figure S2A). Immunoprecipitation experiments showed that SK2 co-immunoprecipitated with UBE3A (Figure 2B, top) and UBE3A co-immunoprecipitated with SK2 (Figure 2B, bottom). Furthermore, the amount of ubiquitinated proteins in SK2 antibody pull-down samples from AS mice was decreased compared to that in WT mice (arrows in Figure 2C). Immunoprecipitation of SK2 by SK2 antibody and ubiquitination of UBE3A were also determined (Figures S2B and S2C). Immunoprecipitation performed under denaturing conditions confirmed that SK2 was ubiquitinated and that its ubiquitination was reduced in AS mice compared to WT mice (arrows in Figure 2D).

### UBE3A Ubiquitinates SK2

To determine whether UBE3A could ubiquitinate SK2 in vitro, we first incubated a purified GST-SK2 C-terminal domain (SK2-C) with ubiquitin, E1, E2, and ATP in the presence or absence of recombinant UBE3A. Under these conditions, UBE3A markedly

increased SK2-C ubiquitination (Figure 3A). The presence of UBE3A and SK2-C was verified by western blots (Figures 3A and S3A).

UBE3A-mediated SK2-C ubiquitination was then confirmed using COS-1 cells transfected with a chimeric construct (Tac-SK2) containing the N-terminal and transmembrane domains of Tac, a constitutively expressed membrane protein (Bonifacino et al., 1990), and the SK2 C terminus. Tac chimeric constructs have been widely used to study membrane protein trafficking (Mu et al., 2003; Standley et al., 2000). Given that COS-1 cells express endogenous UBE3A, we determined the effect of small interfering RNA (siRNA)-mediated knockdown of UBE3A on SK2-C ubiquitination using a His-ubiquitin pull-down assay. COS-1 cells were first incubated with either UBE3A siRNA or a scrambled control siRNA, followed by transfection with Tac-SK2-C and His-ubiquitin. SK2-C ubiquitination was moderately reduced ( $30\% \pm 1\%$  reduction in UBE3A siRNA treated compared to control siRNA treated; p < 0.001, n = 3) following UBE3A siRNA treatment (Figure 3B, bottom), to an extent matching that of UBE3A reduction (Figure 3B, top;  $33\% \pm 4\%$ ; p < 0.01, n = 3). In contrast, overall protein ubiquitination was not affected (Figure S3B). We repeated the experiments with full-length SK2 (SK2-FL) and obtained similar results (Figure S3C). Thus, results from direct ubiquitination assay and His-ubiquitin pull-down analysis showed that SK2 is ubiquitinated in its C terminus by UBE3A.

### Lysine Residues K506, K514, and K550 in the SK2 C-Terminal Domain Are Critical for UBE3A-Mediated Ubiquitination

Multiple lysine residues are present in SK2 C terminus, with several in the calmodulin-binding domain (CaMBD; Figure S3D).

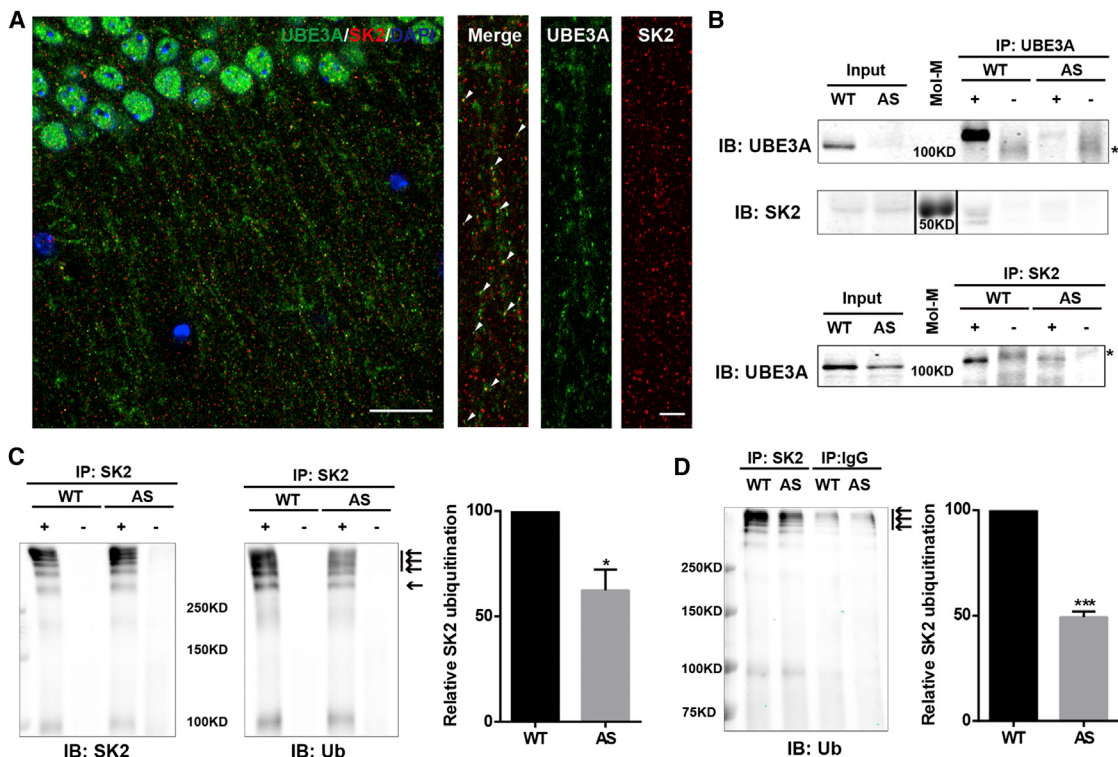


**Figure 2. Interactions between UBE3A and SK2 and SK2 Ubiquitination in Hippocampal Membrane Fractions from WT and AS Mice**

(A) Localization of UBE3A (green) and SK2 (red) in dendritic spines along apical dendrites of CA1 pyramidal neurons from a WT mouse (arrowheads indicate clear co-localization). Scale bar represents 20 μm (left) or 5 μm (right).

(B) Interactions between UBE3A and SK2 in hippocampal P2 fractions. Top: western blot analysis with anti-UBE3A and -SK2 antibodies of immunoprecipitation performed with anti-UBE3A antibodies (+) or control immunoglobulin G (IgG) (-). SK2 is clearly co-immunoprecipitated with UBE3A in WT mice. Bottom: immunoprecipitation was performed with anti-SK2 antibodies, and western blots were labeled with anti-UBE3A antibodies. UBE3A is co-immunoprecipitated with SK2 in WT mice and in AS mice, albeit with reduced amount. Asterisk indicates non-specific bands in control IgG groups. Mol-M, molecular weight marker.

(C) Immunoprecipitation was performed with anti-SK2 antibodies, and western blots were labeled with anti-SK2 and -ubiquitin (Ub) antibodies. Arrows indicate ubiquitinated SK2 and/or SK2-associated proteins.

Right: quantification of the relative abundance of ubiquitinated SK2 and/or SK2-associated proteins in hippocampus of WT and AS mice (mean ± SEM, \*p < 0.05 compared to WT mice, n = 3, Student's t test).

(D) Immunoprecipitation under denaturing conditions was performed with anti-SK2 antibodies or control IgG and western blots were labeled with anti-ubiquitin antibodies. Arrows indicate ubiquitinated SK2. Right: quantification of the relative abundance of ubiquitinated SK2 in hippocampus of WT and AS mice (mean ± SEM, \*\*\*p < 0.001 compared to WT mice, n = 3, Student's t test).

See also Figure S2.

Given that calmodulin is constitutively bound to CaMBD, we targeted the three lysine residues after the CaMBD (Figure 3C). Of note, in silico molecular docking showed that K506 and K514, which are present in the crystal structure of the SK2 C-terminal helix, face the binding groove of UBE3A, where C604, C737, and the catalytic C820 are located (Figure 3D). We simultaneously mutated residues K506, K514, and K550 to alanine ( $\Delta$ K) in Tac-SK2-C and co-transfected this construct in COS-1 cells with either wild-type UBE3A (UBE3A) or its inactive form UBE3A-C833A (Kumar et al., 1999) (referred to as  $\Delta$ UBE3A hereafter) to determine whether these mutations affected SK2-C ubiquitination and whether ubiquitination was also influenced by the amount of functional UBE3A. Tac-SK2-C co-immunoprecipitated with UBE3A and much less with  $\Delta$ UBE3A (Figure S3E), suggesting that interaction between functional UBE3A and SK2 C terminus is involved in SK2 ubiquitination. The His-ubiquitin pull-down assay showed that co-transfection with UBE3A, but

not  $\Delta$ UBE3A, resulted in massive SK2-C ubiquitination, which was significantly reduced by K-A mutation (84% ± 5% reduction compared to UBE3A/Tac-SK2-C group; p < 0.001, n = 3) (Figure 3E, bottom). Again, overall protein ubiquitination was not affected (Figure S3F). These results confirmed that SK2s are ubiquitinated by UBE3A at K506/K514/K550 in the C-terminal domain.

To test whether these lysine residues are also involved in UBE3A-mediated ubiquitination in vivo, we synthesized two short peptides around K550 (PM101 and PM102; see Experimental Procedures). We first tested whether these peptides could disrupt the interaction between SK2 and UBE3A in P2 fractions of hippocampus from WT mice. Immunoprecipitation experiments showed that the amount of SK2 in UBE3A antibody pull-down products was decreased by incubation with peptides PM101 and PM102 at 50 μM (Figure 3F). Immunoprecipitation of UBE3A by UBE3A antibody was also determined (Figure 3F). To

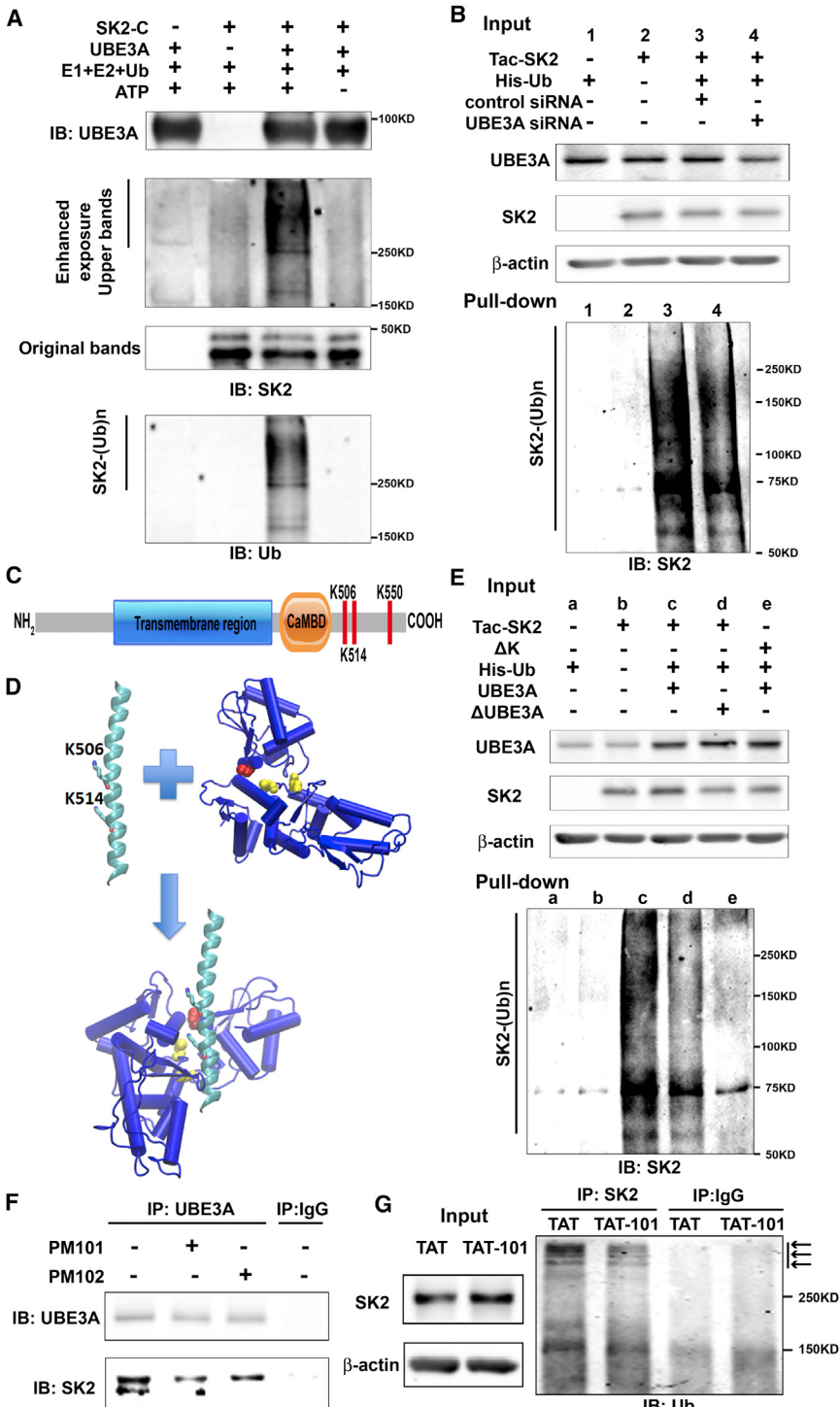


**Figure 3. UBE3A Ubiquitinates SK2 in the C-Terminal Domain**

(A) In vitro ubiquitination of SK2 by recombinant UBE3A. Reaction products were analyzed by western blot with UBE3A (top), SK2 (middle), or ubiquitin (Ub, bottom) antibodies. Note that ubiquitin and SK2 dually labeled high molecular bands (SK2-(Ub)n) are present only when all reaction elements and ATP were added.

(B) siRNA knockdown of UBE3A in COS-1 cells reduces SK2 ubiquitination. COS-1 cells were incubated with UBE3A siRNA or scrambled control siRNA 24 h before transfection with Tac-SK2 and His-ubiquitin. Twenty-four h later, ubiquitinated proteins were isolated by Co<sup>2+</sup>-affinity chromatography. Levels of ubiquitinated Tac-SK2 protein (SK2-(Ub)n, bottom) were determined by western blot. Levels of input proteins were also evaluated by western blot probed with UBE3A, SK2, and β-actin antibodies (top).

(C) Candidate UBE3A ubiquitination sites (K506/K514/K550) within SK2 C terminus. CaMBD, calmodulin-binding domain.

(D) Docking of SK2 C-terminal helix (PDB: 2PNV, chain A 488–526) into UBE3A (PDB: 1D5F). K506 and K514 in the SK2 C-terminal helix are shown in stick representation. C604 and C737 in the larger N-terminal lobe of UBE3A are shown as yellow balls, and catalytic C820 in the smaller C-terminal lobe is shown in red.

(E) K506A/K514A/K550A (ΔK) mutations in SK2 block UBE3A-mediated SK2 ubiquitination. UBE3A overexpression enhances and K506A/K514A/K550A mutations block SK2 ubiquitination in COS-1 cells. His-tagged ubiquitinated proteins in cells co-transfected with either Tac-SK2 plus UBE3A or ΔUBE3A or ΔK plus UBE3A were precipitated using Talon resin and probed with anti-SK2 antibody (bottom). Ubiquitinated SK2 are labeled with "SK2-(Ub)n." Top: input of UBE3A, SK2, and β-actin.

(F) Binding of SK2 with UBE3A is interrupted by PM101 and PM102 peptides. Hippocampal P2 fractions from WT mice were incubated in the presence or absence of PM101 or PM102 (50 μM) peptides followed by immunoprecipitation with either anti-UBE3A antibodies or control IgG. Western blots were performed with anti-UBE3A or anti-SK2 antibodies. Levels of SK2 co-immunoprecipitated with UBE3A were decreased by peptides PM101 or PM102.

(G) Binding of SK2 with UBE3A and its ubiquitination in vivo were disrupted by systemic administration of the TAT-101 peptide. WT mice were injected with either control TAT or TAT-101 (i.p. 50 mg/kg), and hippocampi were collected 2 hr later for immunoprecipitation and western blot. Immunoprecipitation under denaturing conditions

was performed with anti-SK2 antibodies or control IgG, and western blots were labeled with anti-ubiquitin antibodies (right). Arrows indicate ubiquitinated SK2. See also Figure S3.

allow for efficient delivery of the peptide across the blood-brain barrier, we conjugated PM101 to the cell membrane transduction domain of HIV-1 Tat protein (TAT-101). It is well established

that peptides/proteins that are fused to TAT are rapidly and efficiently introduced into live tissues when systemically administered into intact animals while retaining their biological activity

(Rapoport and Lorberbaum-Galski, 2009; Xu et al., 2007). Four-month-old WT mice were injected with either control TAT or TAT-101 (intraperitoneally [i.p.], 50 mg/kg) and hippocampi collected 2 hr later. Western blot results showed that SK2 levels in P2 fractions were significantly increased following TAT-101 treatment ( $11\% \pm 3\%$ ;  $p < 0.01$ ,  $n = 4$ ) compared to TAT control (Figure 3G). Immunoprecipitation performed under denaturing conditions confirmed that SK2 ubiquitination was also reduced in TAT-101-treated mice ( $30\% \pm 3\%$ ,  $p < 0.001$ ;  $n = 3$ ) compared to control TAT-treated mice (arrows in Figure 3G). These results indicate that sequences around K550 in the SK2 C-terminal domain are critical for both interaction with and ubiquitination by UBE3A in vivo.

#### UBE3A-Mediated Regulation of SK2 Surface Expression and Endocytosis Depends on K506/K514/K550

To further understand the role of UBE3A-mediated SK2 ubiquitination, we analyzed SK2 surface expression and endocytosis first in COS-1 cells. Tac-SK2 surface expression, detected with a Tac-specific antibody, was significantly reduced following co-transfection with UBE3A but was markedly increased following  $\Delta$ UBE3A co-transfection (Figures 4A and 4B, left; Figure S4A). In contrast, co-transfection with either UBE3A or  $\Delta$ UBE3A did not affect surface expression of a similar construct consisting of Tac and the C-terminal domain of the AMPA receptor (AMPAR) subunit, GluA2 (Tac-GluA2; Figure S4B). Results similar to those obtained with Tac-SK2 were obtained with full-length SK2 (Figure S4C). The effects of UBE3A and/or  $\Delta$ UBE3A on Tac-SK2 surface expression were also confirmed by western blots from cell membrane fractions, although co-transfection of Tac-SK2 with UBE3A or  $\Delta$ UBE3A did not significantly alter SK2 levels in whole homogenates (Figure S4D). K-A mutation at K506/K514/K550 ( $\Delta$ K) significantly increased surface expression and eliminated the effect of UBE3A (Figure 4A, right; and Figure 4B, left). In endocytosis assays, UBE3A significantly increased, while  $\Delta$ UBE3A significantly reduced, Tac-SK2 internalization (Figures 4A, left, and 4B, right; Figure S4E). K-A mutation significantly reduced SK2 endocytosis and eliminated the effect of UBE3A (Figures 4A and 4B, right). Similar results were obtained when lysine residues K506/K514/K550 were changed to arginine ( $\Delta$ K2; Figure S4E). These results suggest that UBE3A facilitates SK2 endocytosis, possibly by ubiquitination of K506/K514/K550 residues.

To determine whether UBE3A-mediated regulation of SK2 surface expression and endocytosis in COS-1 cells also occurred in neurons, we cultured hippocampal neurons from AS and WT embryos. We first confirmed that SK2 levels were higher in membrane fractions from cultured hippocampal neurons of AS mice compared to WT mice (Figure 4C). We then performed biotinylation assay to detect surface-expressed and internalized SK2s in cultured hippocampal neurons. The results showed that levels of membrane-associated SK2s were significantly higher in AS neurons than in WT neurons (Figure 4D). While significant amounts of SK2s were detected in the endocytotic fraction from WT neurons, SK2s were barely detectable in the similar fraction from AS mice neurons (Figure 4D). In contrast, GluA1 was detectable in the endocytotic fraction from both WT and AS mice (Figure 4D). These results reveal a specific UBE3A-

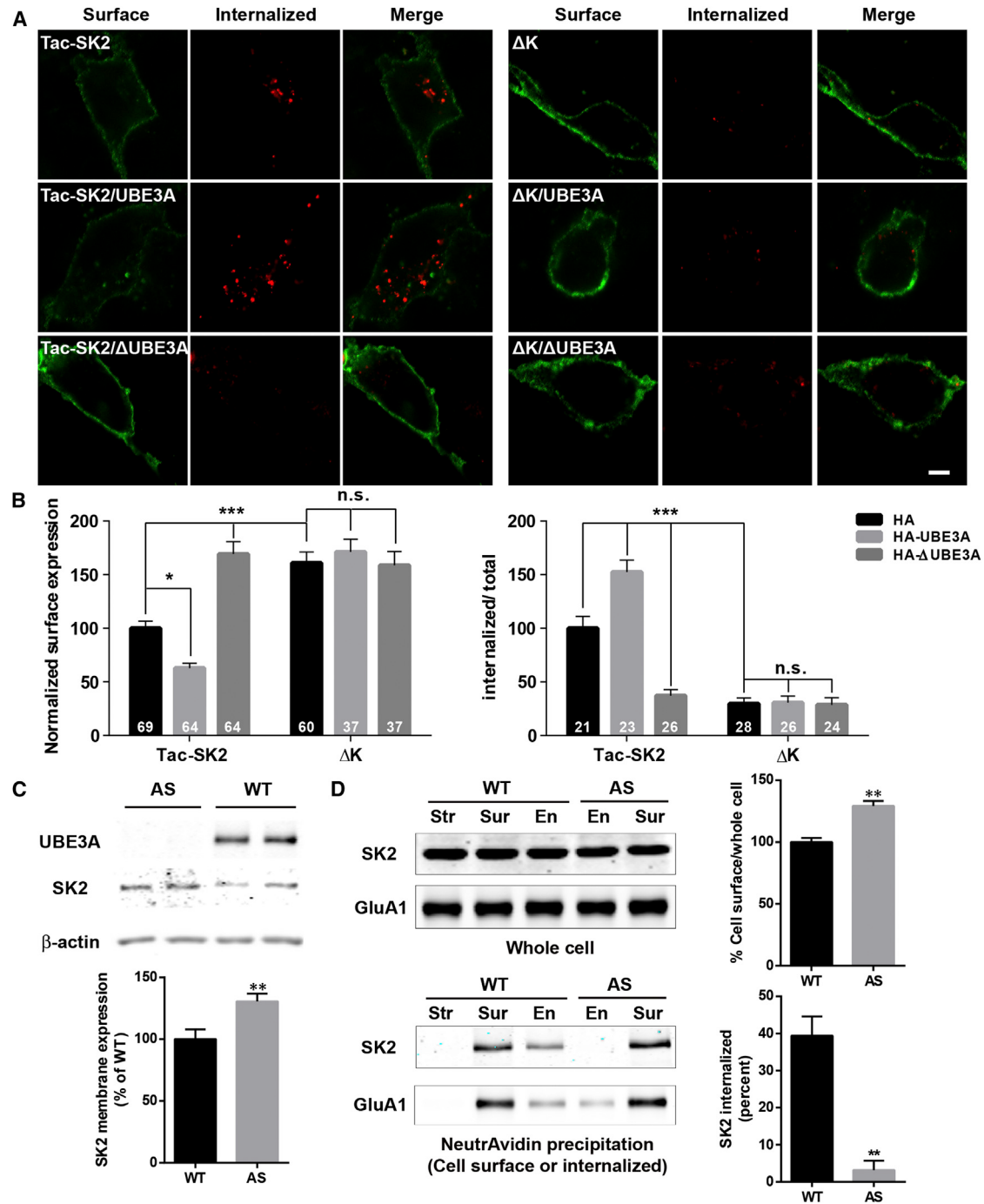
dependent regulation of SK2 endocytosis in hippocampal neurons.

#### Increased SK2s Result in Synaptic Plasticity Impairment and Decreased NMDAR Function in AS Mice

To determine whether changes in SK2 synaptic expression contributed to LTP impairment in AS mice, we determined the effects of apamin, a selective SK2 blocker, on LTP in acute hippocampal slices. As previously reported, theta-burst stimulation (TBS) induced LTP in field CA1 of hippocampal slices in WT mice, whereas it elicited only transient facilitation in AS mice (Figures 5A and 5B, red trace). Following pre-incubation of hippocampal slices from AS mice with apamin (20 nM), TBS-elicited LTP was identical to that in WT mice (Figures 5A and 5B, blue trace). Apamin at this concentration did not affect TBS-induced LTP in slices from WT mice (Figures 5A and 5B, pink trace), nor did it affect baseline synaptic responses or responses in a control pathway (Figures 5A, 5B, and S5A) or paired-pulse facilitation (Figure S5B) in slices from either WT or AS mice.

Like LTP, long-term depression (LTD) of synaptic transmission is also generally assumed to be involved in learning and memory. We therefore determined whether LTD was altered in AS mice. Low-frequency stimulation (LFS; 1 Hz, 15 min) of the Schaffer collaterals in hippocampal slices from 3-month-old WT mice induced a transient synaptic depression, and synaptic responses slowly returned to baseline levels (Figure 5C, white circle, top), a result consistent with the literature (Dudek and Bear, 1993). However, the same protocol induced sustained LTD in slices from 3-month-old AS mice (Figure 5C, red circle in top). Apamin (20 nM) pre-treatment significantly reduced LTD in AS mice (Figures 5C and 5D, blue in the top) and did not affect responses to low-frequency stimulation in slices from WT mice. Since induction of both LTP and LTD at Schaffer collateral-CA1 synapses is NMDAR dependent and SK2-mediated hyperpolarization inhibits NMDAR-channel opening, we analyzed the effect of apamin treatment on NMDAR-mediated synaptic responses ( $\text{NfEPSPs}$ ).  $\text{NfEPSPs}$  were isolated by bath application of a  $\text{Mg}^{2+}$ -free ACSF containing 6-cyano-7-nitroquinoxaline-2,3-dione (CNQX; 10  $\mu\text{M}$ ) to block AMPA-receptor-mediated synaptic transmission. The NMDAR antagonist AP5 was used to verify that  $\text{NfEPSPs}$  were mediated by NMDARs under these conditions (Figure 5E).  $\text{NfEPSP}$  amplitudes were significantly lower in AS mice compared to WT mice, and this decrease was reversed by apamin application (Figures 5F, 5G, and S5C), suggesting that SK2 imposes a stronger inhibition of NMDAR in AS mice than in WT mice. At this concentration, apamin did not significantly increase  $\text{NfEPSP}$  in WT mice (Figures 5F and 5G). AP5 pre-treatment also significantly reduced LTD in AS mice (Figure S5D), suggesting that the enhanced LTD in AS mice is also NMDAR dependent.

To confirm that increased SK2 activity was due to the lack of UBE3A-mediated regulation, we determined the effect of the TAT-101 peptide on LTP induction in WT mice. Hippocampal slices were prepared 2 hr after administration of either control TAT or TAT-101 peptide (i.p., 50 mg/kg). In hippocampal slices from TAT-101-treated mice, TBS induced only a transient enhancement in synaptic responses, as found in slices from AS mice.

**Figure 4. UBE3A Regulates SK2 Surface Expression and Endocytosis in COS-1 Cells and Cultured Hippocampal Neurons**

(A and B) Effects of UBE3A overexpression and K-A mutation on SK2 surface expression and endocytosis. (A) Representative images of internalized (red) or surface-expressed (green) Tac-SK2 (left) and ΔK (right) in COS-1 cells co-transfected with HA (top), HA-UBE3A (middle), or HA-ΔUBE3A (bottom). Scale bar, 10 μm. (B) Quantitative analysis of images in (A). Data are expressed as mean ± SEM. \*p < 0.05, \*\*p < 0.01, and \*\*\*p < 0.001 compared to Tac-SK2/HA (Tac-SK2); two-way ANOVA with Newman-Keuls post hoc analysis. n is indicated in each column and from at least three independent experiments.

(C and D) Regulation of SK2 membrane expression and internalization by UBE3A in cultured hippocampal neurons. (C) Top: representative blots of UBE3A, SK2, and β-actin in P2 fractions. Bottom: quantitative data (mean ± SEM; n = 10–11 E18 mouse embryos; unpaired Student's t test, \*\*p < 0.01). (D) Biotinylation assays of SK2 and GluA1 (used as control) endocytosis with hippocampal neurons. Biotinylated SK2 and GluA1 were isolated by NeutrAvidin precipitation and detected by western blot with SK2 and GluA1 antibodies (lower left). Upper left: levels of SK2 and GluA1 in whole homogenate (input). Upper right: ratio

(legend continued on next page)

In contrast, LTP was intact in hippocampal slices from control TAT-treated mice (Figures 5H and 5I).

We previously showed that LTP impairment in AS mice was associated with reduced actin polymerization following TBS application (Baudry et al., 2012). Therefore, we determined the effect of apamin application on TBS-induced actin polymerization using Alexa-Fluor-568-conjugated phalloidin, which selectively binds to filamentous actin (F-actin). TBS elicited a clear increase in the number of F-actin-positive puncta in WT slices, but not in AS slices. Apamin pre-treatment markedly enhanced TBS-induced actin polymerization in AS slices (Figure S6).

### Increased SK2s Alter TBS-Induced LTP Properties in AS Mice

Recent studies have revealed that TBS-induced LTP is followed by a refractory period (~1 hr) during which another TBS cannot enhance LTP magnitude, while multiple TBS trains separated by longer time intervals are able to increase LTP magnitude (Kramár et al., 2012). This LTP property was tested in hippocampal slices from AS mice by applying a second TBS (TBS2) train at 10, 45, or 60 min after the first TBS (TBS1). As previously reported (Lynch et al., 2013), TBS2 applied 10 min (Figure 6B) post-TBS1 in WT hippocampal slices failed to further enhance LTP magnitude, while after 60 min (Figure 6A), TBS2 significantly increased LTP magnitude. In contrast, TBS2 applied at 10 min (Figure 6B) or 45 min (Figures S7A and S7B) after TBS1 in AS hippocampal slices significantly enhanced LTP magnitude to a level comparable to that found in WT mice. In addition, when applied 60 min (Figure 6A) after TBS1, TBS2 failed to significantly increase LTP.

Quantitative image analysis showed that TBS1 stimulation induced a significant reduction in the percentage of SK2-immunopositive synapses in WT mice, a result in good agreement with a previous study (Lin et al., 2008). In AS mice, TBS1, although unable to induce LTP, produced a similar reduction in the percentage of SK2-immunopositive synapses, suggesting that TBS1-elicited SK2 internalization enables TBS2 to induce LTP shortly after TBS1 (Figures 6D and 6E). This idea was further supported by the fact that following pre-incubation with apamin in AS slices, TBS2 applied 10 min after TBS1 did not further enhance LTP (Figure 6C).

### Treatment with Apamin Improves Learning and Memory Performance of AS Mice in the Fear-Conditioning Paradigm

To determine whether apamin could also reverse impairment in hippocampus-dependent learning in AS mice, we used the fear-conditioning paradigm. AS and WT mice were injected with apamin (0.4 mg/kg, i.p.) 30 min before the training session, as previously reported (Vick et al., 2010). AS mice were impaired in a context-dependent fear conditioning and tone test, and apamin treatment significantly enhanced learning performance in AS mice (Figure 7). Under our experimental conditions (three condi-

tioned stimuli [CS] paired with three unconditioned stimuli [US]), apamin treatment did not affect learning in WT mice. Additionally, there was no difference in freezing time in the pre-conditioning period, during training, or before tone application in the testing period among all experimental groups (Figure S7C).

## DISCUSSION

Our results indicate that UBE3A-mediated regulation of synaptic SK2s plays critical roles in synaptic plasticity and learning and memory. SK2 and UBE3A were co-localized in dendrites and spines of hippocampal pyramidal neurons, and lack of UBE3A resulted in increased synaptic SK2 levels and decreased SK2 ubiquitination. SK2 was ubiquitinated by UBE3A at residues K506/K514/K550 in its C-terminal domain, resulting in SK2 internalization. Both the interaction between SK2 and UBE3A and SK2 ubiquitination were significantly reduced by small peptides that comprise the SK2 C-terminal sequence around residue K550. Electrophysiological studies revealed that increased SK2 levels imposed a tonic inhibition of NMDARs, accounting for impairments in TBS-induced LTP and actin polymerization in hippocampal slices from AS mice. The interaction-disrupting peptide TAT-101 produced LTP impairment in slices from WT mice, similar to that observed in AS mice. In vivo experiments demonstrated that increased synaptic SK2 levels also contributed to learning and memory deficits in the fear-conditioning paradigm. Together, these results not only indicate that SK2 is a substrate of UBE3A but also reveal a mechanism by which UBE3A regulates synaptic plasticity and cognitive functions.

### UBE3A Ubiquitinates SK2s in Their C-Terminal Domain, Resulting in Their Endocytosis

Several synaptic proteins are regulated by the ubiquitin-proteasome system (for recent reviews, see Lin and Man, 2013; Mabb and Ehlers, 2010). For instance, PSD-95 is ubiquitinated by the E3 ligase Mdm2 leading to subsequent degradation by proteasomes in response to NMDAR activation (Colledge et al., 2003). PSD-95 ubiquitination also results in increased AMPAR internalization, possibly through a non-proteolytic function, i.e., by interacting with and enhancing clathrin-dependent endocytosis (Bianchetta et al., 2011). Both NMDARs and AMPARs are also modified by protein ubiquitination; the NMDAR subunit GluN2B is ubiquitinated by the RING family E3 ligase Mib2 (Jurd et al., 2008), the AMPAR subunit GluA1 by Nedd4 (Lin et al., 2011), and GluA2 by an undefined E3 ligase (Lussier et al., 2011). Our results add to this list another member of post-synaptic proteins by showing that UBE3A ubiquitinates SK2 in its C-terminal domain, on lysine residues K506, K514, and K550. Mutations of these lysine residues to either alanine or arginine not only reduced SK2 channel endocytosis and increased their surface expression but also eliminated UBE3A-mediated SK2 ubiquitination and endocytosis. Finally, the endocytosis-biotinylation assay showed that, whereas SK2 was detectable in

(mean ± SEM of three independent experiments) of surface-expressed SK2 over total SK2. Lower right: ratio (mean ± SEM of three independent experiments) of internalized SK2 over surface-expressed SK2. \*\* $p < 0.01$ , unpaired Student's t test. Str, samples from stripped dish; Sur, total surface proteins; En, internalized proteins.

See also Figure S4.

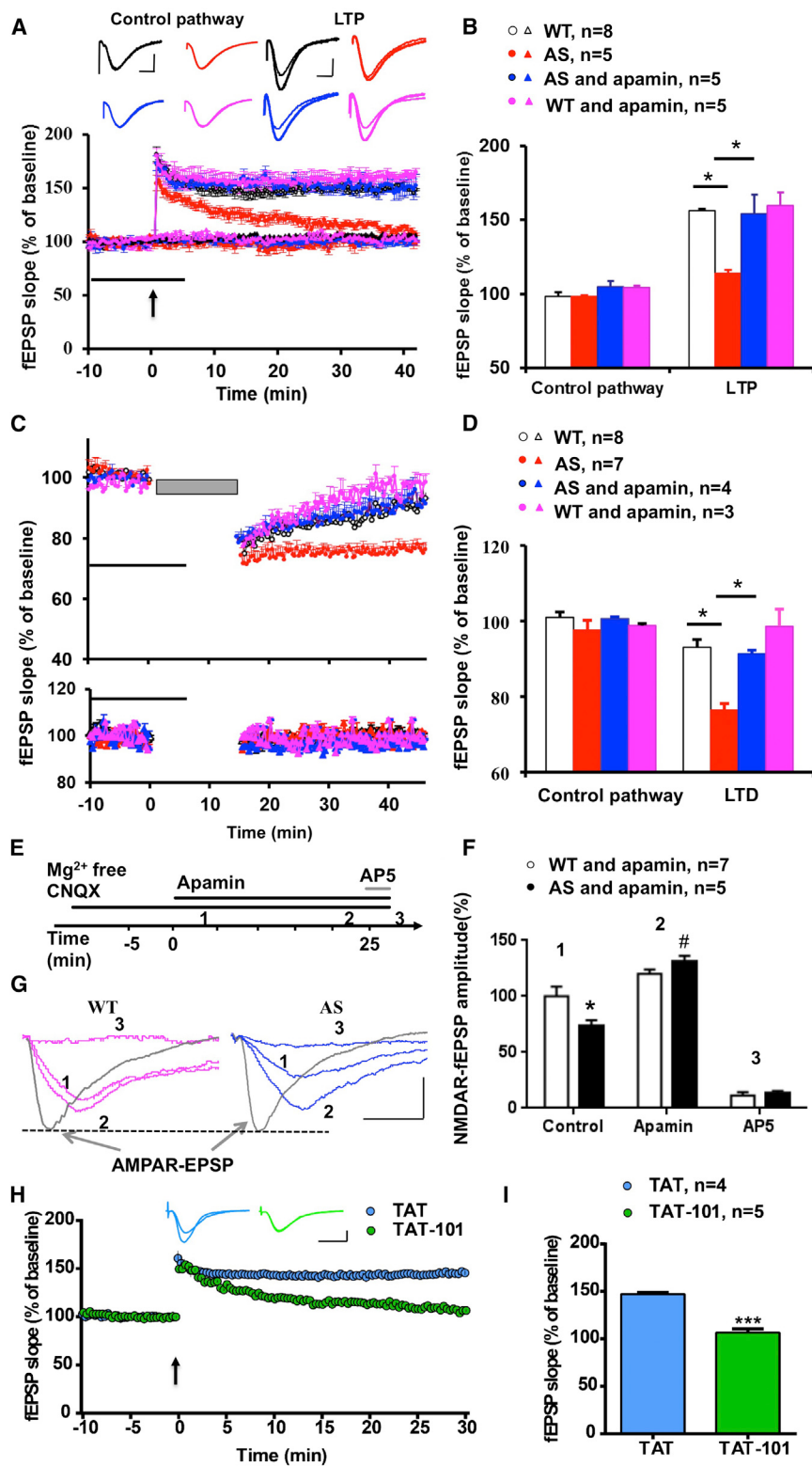


**Figure 5. Impairment of NMDAR-Dependent Hippocampal Synaptic Transmission and Activity-Dependent Synaptic Plasticity in Hippocampal Slices from AS Mice**

(A) Reversal of LTP impairment in AS mice by apamin, an SK2 channel blocker. Slopes of field excitatory postsynaptic potential (fEPSPs) were normalized to the average values recorded during the 10-min baseline. Insert shows representative traces of evoked fEPSPs before and 40 min after TBS (arrow). Scale bar, 0.5 mV/10 ms.

(B) Mean  $\pm$  SEM of fEPSPs (expressed as % of WT control pathway) measured 40 min after TBS in different groups. \*p < 0.05 (one-way ANOVA followed by Bonferroni test).

(C) LTD in hippocampal slices from AS mice is blocked by apamin. Top: LTD induced by LFS (1 Hz for 15 min). Bottom: effect of apamin on control pathway.

(D) Mean  $\pm$  SEM of fEPSPs measured 40 min after LFS in different groups. \*p < 0.05 (one-way ANOVA followed by Bonferroni test).

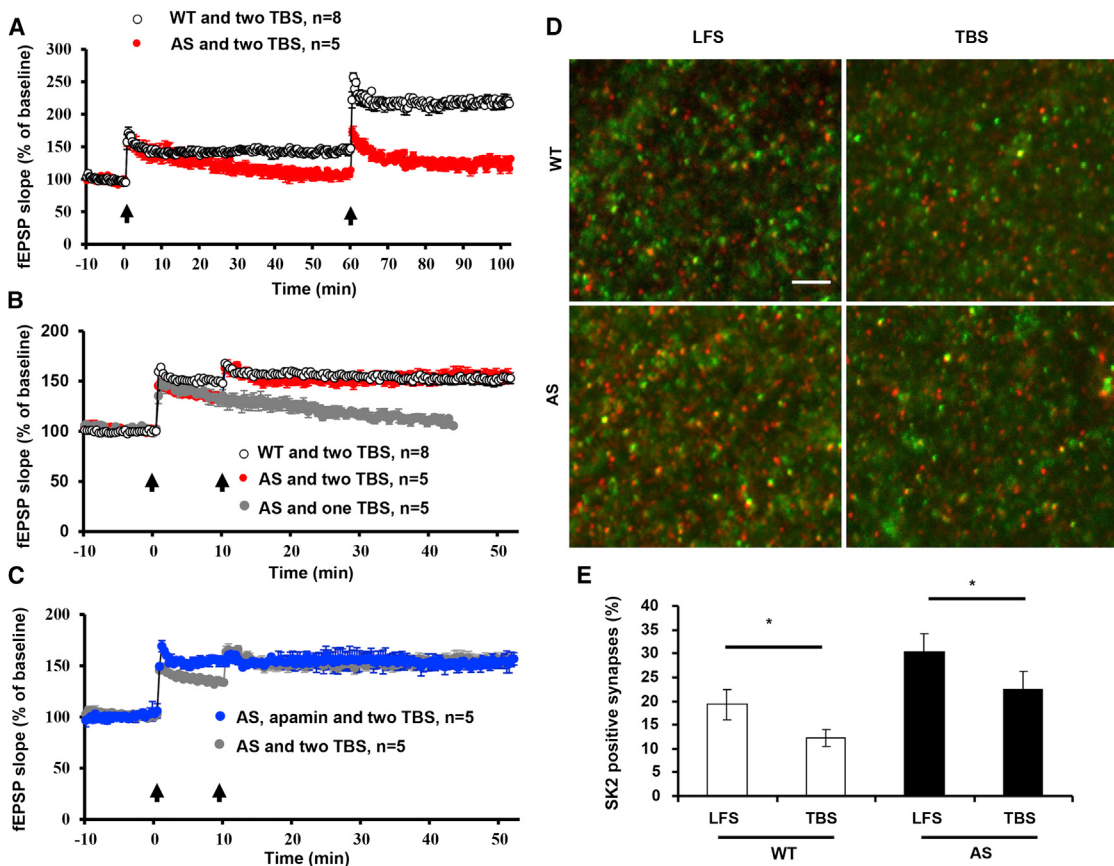
(E) Protocol and time points used for analysis of NMDAR-mediated synaptic transmission (NfEPSP).

(F and G) Representative traces (G) and quantification of NfEPSPs (F) recorded at the time points indicated in (E). Data are means  $\pm$  SEM expressed as % of values in WT hippocampal slices before apamin treatment (WT control); \*p < 0.05 compared to WT control; #p < 0.05 compared to AS control (two-way ANOVA followed by Bonferroni test). Traces of AMPAR fEPSPs indicate that synaptic responses before initiation of NfEPSP recording are similar between AS and WT mice. Scale bar, 0.5 mV/20 ms.

(H) Systemic injection of peptide TAT-101 impaired LTP induction in WT mice. Insert shows representative traces of evoked fEPSPs before and 30 min after TBS (arrow). Scale bar, 0.5 mV/10 ms.

(I) Mean  $\pm$  SEM of fEPSPs measured 30 min after TBS in the two groups. \*\*\*p < 0.001 (Student's t test).

See also Figures S5 and S6.

**Figure 6. UBE3A-Deficiency-Induced Changes in LTP Properties**

(A) Two TBS (arrows) separated by 60 min could induce further potentiation in hippocampal slices from WT mice, while neither the first or second TBS induced LTP in hippocampal slices from AS mice.

(B) A second TBS(2) applied 10 min after the first TBS(1) did not induce further potentiation in slices from WT mice. However, the same TBS2 was able to induce LTP in hippocampal slices from AS mice.

(C) With apamin pre-application, TBS2 applied 10 min post TBS1 was not able to further enhance LTP in AS mice.

(D) TBS elicited a decrease in the number of SK2-positive synapses in both WT and AS mice. Shown are representative images of SK2 (red) and PSD95 (green) immunostaining in the CA1 region of WT and AS mice (Scale bar, 10  $\mu$ m).

(E) Quantitative results (mean  $\pm$  SEM) of synapses dually labeled by anti-SK2 and anti-PSD95 antibodies in different experimental groups (\* $p < 0.05$ , n = 3 slices from three mice/group, one-way ANOVA followed by Bonferroni test).

See also Figure S7.

both cell membrane and endocytic fractions in neurons cultured from WT mice, it was only observed in cell membrane fractions in neurons from AS mice, suggesting that UBE3A deficiency impairs tonic SK2 endocytosis. The reduction in SK2 endocytosis could account for the increased SK2 levels in crude synaptosomal and PSD fractions found in hippocampus of AS mice.

#### Roles of UBE3A-Mediated SK2 Regulation in Synaptic Plasticity

We previously reported that a semi-chronic treatment with an AMPAR-positive regulator, CX929, reversed LTP impairment in AS mice, possibly due to increased brain-derived neurotrophic factor (BDNF) production. In the current study, we showed that acute apamin application in hippocampal slices was able to restore TBS-induced LTP in AS mice. BDNF has been shown

to facilitate NMDAR-mediated LTP, and, as we discussed, apamin treatment also increases NMDAR activity. Thus, CX929 and apamin treatments converge on NMDARs and possibly on downstream signaling pathways as well, since both CX929 treatment and apamin application were able to restore actin polymerization in dendritic spines following LTP induction. We therefore argue that LTP impairment in AS mice takes place at the induction phase, possibly due to insufficient NMDAR activation, and we postulate that any manipulation that enhances LTP induction could be beneficial to re-establish normal synaptic plasticity in AS mice. In addition, treatments bypassing the induction stage and directly activating downstream signaling cascades, such as increasing CaMKII activity (van Woerden et al., 2007) or promoting cytoskeletal remodeling (Baudry and Bi, 2013; Lynch et al., 2008), could be beneficial as well.

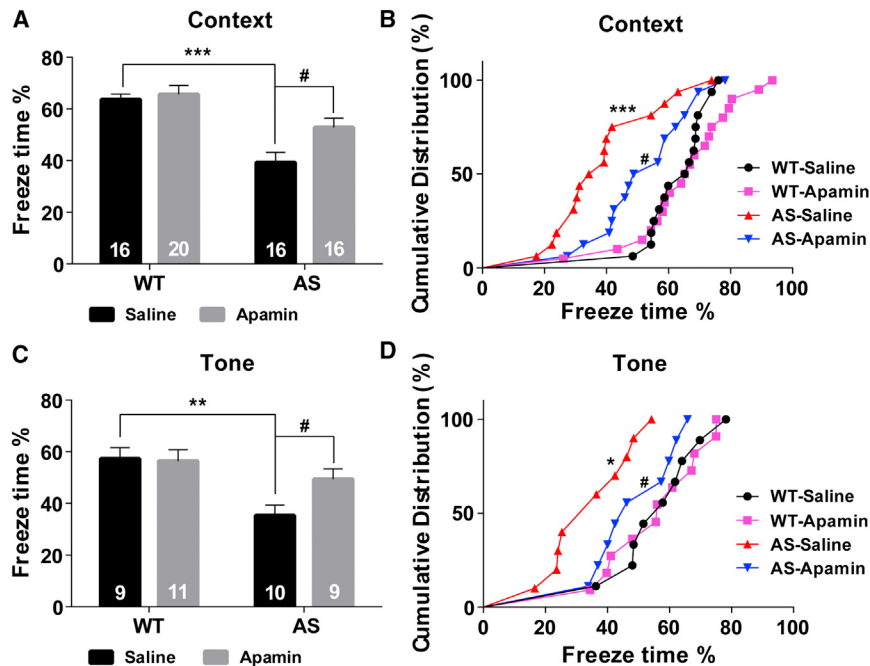


**Figure 7. Effects of Apamin Treatment on Fear Conditioning in WT and AS Mice**

(A) Percent freezing for different experimental groups in context memory (mean  $\pm$  SEM of 16–20 mice; \*\*\* $p$  < 0.001 compared to WT controls; # $p$  < 0.05 compared to vehicle-treated AS mice; two-way ANOVA with Newman-Keuls post hoc analysis).

(B) Cumulative distribution of % freezing in WT and AS mice treated with vehicle or apamin assessed by the Kolmogorov-Smirnov test in context memory (\*\* $p$  < 0.001 compared to WT controls; # $p$  < 0.05 compared to vehicle-treated AS mice).

(C and D) Cumulative distribution and % freezing for different experimental groups in tone memory (mean  $\pm$  SEM of 9–11 mice; \* $p$  < 0.05 and \*\* $p$  < 0.01 compared to WT controls; # $p$  < 0.05 compared to vehicle-treated AS mice). See also Figure S7.

SK2 upregulation in hippocampal CA1 synapses could be responsible for LTD induction in adult AS mice. A recent study reported that mGlu5-receptor-mediated LTD was also enhanced in AS mice

(Pignatelli et al., 2014). Of notice, mGlu5 receptors and SK2s have been shown to form a reciprocally regulating complex (García-Negredo et al., 2014). Thus, it is possible that increased synaptic SK2 levels contribute to mGlu5-receptor-mediated LTD enhancement, and this question will be investigated in future studies.

#### Role of UBE3A-Mediated Regulation of SK2s in Learning and Memory

Previous studies, including our own, showed that, compared with their WT littermates, AS mice exhibit a clear deficit in context-dependent fear conditioning (Baudry et al., 2012; Jiang et al., 1998; van Woerden et al., 2007). We previously showed that a semi-chronic treatment with CX929 reversed the behavioral deficit and re-established normal levels of freezing in response to context and cue (Baudry et al., 2012). Manipulations of SK2 activity have been shown to influence learning performance in various paradigms (Deschaux et al., 1997; McKay et al., 2012; Stackman et al., 2002). A recent study showed that apamin enhanced contextual fear memory in WT mice conditioned with one CS-US pairing protocol, but not with three CS-US pairings (Vick et al., 2010). In the present study, we used a three CS-US pairing protocol, and under this condition, apamin had no effect on fear-conditioning learning in WT mice but significantly improved both context- and cue-dependent learning in AS mice. These results support our hypothesis that in AS mice, increased levels of synaptic SK2s are responsible for hippocampal-dependent learning deficit. In summary, our results suggest that synaptic SK2 endocytosis is directly regulated by UBE3A-mediated ubiquitination and that this regulation is critically involved in synaptic plasticity and learning performance, while defects in this regulation could contribute to intellectual disability, as seen in AS.

Recently, a series of studies has revealed that LTP has a refractory period lasting ~1 hr after TBS (Lynch et al., 2013). We recently found that two different isoforms of the calcium-activated protease, calpain, play a critical role in LTP induction and the initiation of the refractory period (Wang et al., 2014). These findings provide a biological basis for the widely recognized phenomenon that new information is better retained with spaced-trial learning than with massed-trial learning (Benjamin and Tullis, 2010). In the present study, we found that at intervals  $\leq$ 45 min, TBS2 was able to induce LTP in AS mice, suggesting that a short lasting process triggered by TBS1 was sufficient for facilitating LTP induction in AS mice. Since TBS2 delivered at 10-min intervals did not further enhance LTP in apamin pretreated slices, it is possible that removal of SK2 channels by TBS1 contributes, at least partly, to the reinstatement of LTP by TBS2 delivered shortly after TBS1 in hippocampal slices from AS mice. Our immunofluorescence results support the notion that TBS1 induces SK2 internalization. Lin et al. also proposed that LTP-induced SK2 internalization depended on PKA-mediated phosphorylation and that direct SK2 phosphorylation in the C-terminal domain may initiate its endocytosis (Lin et al., 2008; Ren et al., 2006). Whether TBS1-induced SK2 removal in AS mice also depends on PKA activation and whether this process interacts with UBE3A-mediated SK2 ubiquitination are currently under investigation.

LTD has been reported to be impaired in layer 2/3 synapses in visual cortex in adult AS mice, although LTD is reliably induced in these synapses in adult WT mice (Yashiro et al., 2009). In contrast, it is difficult to reliably introduce LTD in the adult hippocampus (Dudek and Bear, 1993), and our results showed that this is the case in adult WT mice. However, stable LTD was induced in hippocampal slices from AS mice, which was blocked by apamin application. These results suggest that

## EXPERIMENTAL PROCEDURES

### Mice

Animal experiments were conducted with protocols approved by the local institutional animal care and use committee. Original UBE3A mutant (AS) mice were obtained from The Jackson Laboratory (strain 129-Ube3a<sup>tmt1Ab/J</sup>), and a breeding colony was established as previously described (Baudry et al., 2012). In all experiments, male AS mice and WT littermates between 2 and 4 months of age were used.

### Hippocampal Neuronal Cultures

Hippocampal neurons were prepared from embryonic day 18 (E18) mouse embryos, bred with UBE3A<sup>m−/p+</sup> female and male mice, as described previously (Qin et al., 2009).

### Cell Lines

COS-1 cells (ATCC) were grown in DMEM supplemented with 10% (v/v) fetal bovine serum (FBS) (Invitrogen).

### DNA Constructs, Transfection, Antibodies, and Peptides

For transient expression, cells were transfected with the respective constructs and/or siRNA by lipofection (Lipofectamine 2000, Invitrogen).

Details regarding DNA constructs and antibodies can be found in the Supplemental Experimental Procedures.

The following peptides were synthesized by ABI Scientific: PM101 (NYDKHV), PM102 (MENYDKHVSYN), TAT (YGRKKRRQRRR), and TAT-101 (YGRKKRRQRRRNNDKHV).

### Subcellular Fractionation and Western Blot Analysis

Fractionation methods were modified from those of Smith et al. (2006) to yield P2 and P3 fractions relatively enriched in postsynaptic density fractions (PSDs). Western blots were performed according to published protocols (Sun et al., 2015) with IRDye secondary antibodies and detected with the Odyssey imaging system.

### Immunoprecipitation and Denaturing Immunoprecipitation

Immunoprecipitation was performed by incubating hippocampal P2 fractions with appropriate antibodies and agarose beads following standard procedures. For SK2 immunoprecipitation under denaturing conditions, P2 pellets were heated in denaturing lysis buffer, diluted in ice-cold non-denaturing lysis buffer, and then incubated with antibodies coupled to protein A/G agarose beads.

### In Vitro Ubiquitination Assay

GST-SK2 proteins containing the whole SK2 C terminus were expressed in *E. coli* BL21 (DE3) and purified as previously described (Ren et al., 2006). The E6AP (UBE3A) Ubiquitin Ligase Kit (Boston Biochem) containing E1 and E2 enzyme (UBE2D3), His<sub>6</sub>-UBE3A, ubiquitin, Mg<sup>2+</sup>-ATP, and reaction buffer was used. For negative control reactions, ATP was omitted. Three independent experiments were performed.

### His-Ubiquitin Pull-Down Assay

COS-1 cells were transfected with His-ubiquitin plus Tac-SK2 or ΔK and HA-UBE3A or HA-UBE3A C833A constructs, UBE3A, or control siRNA. Twenty-four hours after transfection, cells were lysed, and His-ubiquitin-conjugated proteins were purified as described previously (Xirodimas et al., 2001) with minor modifications.

### In Silico Molecular Docking

In silico molecular docking was performed between the crystal structure of SK2 C-terminal helix (PDB: 2PNV, chain A 488–526) (Kim et al., 2008) and the crystal structure of UBE3A (PDB: 1D5F) (Huang et al., 1999). Patchdock (Duhovny et al., 2002; Schneidman-Duhovny et al., 2005) was used for docking.

### Endocytosis Assay of Tac-SK2 in COS-1 Cells

Analysis of Tac-SK2 internalization was performed as previously reported (Roche et al., 2001; Standley et al., 2000) and detailed in the Supplemental

**Experimental Procedures.** In brief, cultured COS-1 cells were incubated with Tac7G7 antibodies on ice, antibodies bound to Tac-SK2 were allowed to be internalized, and internalized Tac-SK2 and surface-expressed Tac-SK2 were visualized by using two different fluorophore-conjugated secondary antibodies.

### Image Analysis and Quantification

Images were acquired using a Nikon C1 confocal laser-scanning microscope. Acquisition parameters were kept identical among different experimental groups. All immunostaining studies were performed in three to five independent experiments. Tac-SK2 surface expression and internalization were analyzed using ImageJ (NIH).

### Neuronal Biotinylation Assay

Neuronal biotinylation assay was performed as previously reported (Roche et al., 2001) and detailed in the Supplemental Experimental Procedures. In brief, cultured hippocampal neurons were incubated with sulfo-NHS-SS-biotin (Pierce) on ice, and biotinylated proteins were either precipitated with NeutrAvidin Agarose (Pierce) or allowed to be internalized and precipitated after the remaining surface biotin was stripped.

### Acute Hippocampal Slice Preparation, Electrophysiology, and Phalloidin Staining

Acute slice preparation, recordings, and phalloidin staining of F-actin were performed as previously described previously (Baudry et al., 2012; Wang et al., 2014).

### Immunofluorescence of Brain Tissue Sections

For immunofluorescence, brain sections (25 μm) were processed as previously described (Sun et al., 2015; Wang et al., 2014).

### Fear Conditioning

Male AS and WT mice were subjected to fear-conditioning testing as described in the Supplemental Experimental Procedures. On training day, mice were injected i.p. with apamin (0.4 mg/kg) 30 min before training. Training was conducted in a fear-conditioning chamber (H10-11M-TC, Coulbourn Instruments) and behavior was recorded with the Freezeframe software and analyzed with Freezeframe software (Coulbourn Instruments).

### Statistical Analysis

Error bars indicate SEM. To compute p values, an unpaired Student's t test, Kolmogorov-Smirnov test, and one- or two-way ANOVA with Newman-Keuls or Bonferroni post test were used, as indicated in figure legends.

## SUPPLEMENTAL INFORMATION

Supplemental Information includes Supplemental Experimental Procedures and seven figures and can be found with this article online at <http://dx.doi.org/10.1016/j.celrep.2015.06.023>.

## AUTHOR CONTRIBUTIONS

J.S., G.Z., and Y.L. performed most of the experiments and prepared the figures. S.S., A.J., and R.T. prepared constructs used in the experiments. Y.L. and C.C. performed fear-conditioning experiments. Y.W. performed some immunofluorescent experiments. L.L. performed the docking experiment. M.B. worked on the figures and wrote the manuscript. X.B. directed the research, worked on the figures, and wrote the manuscript.

## ACKNOWLEDGMENTS

The authors are grateful to Dr. Gary Lynch for his insightful comments and would like to thank Ms. Stephanie Moreno, Mr. Erik Lee, and Mr. Omar Abouelnasr for helping maintain the mouse colonies; Dr. Guanghong Liao, Mr. Max Zhvanetsky, Mr. Neema Baudry, Ms. Zhuangjun Wang, Ms. Rachana Adhikari, and Dr. Li Qian for their involvement in some of the experiments; and

Drs. Victor Briz and Pen-Jen Lin for helpful discussions. This work was supported by grant MH101703 (to X.B.) and grants NS045260 (PI: Dr. C.M. Gall) and NS057128 (to M.B.). X.B. is also supported by funds from the Daljit and Elaine Sarkaria Chair.

Received: January 5, 2015

Revised: April 30, 2015

Accepted: June 7, 2015

Published: July 9, 2015

## REFERENCES

- Adelman, J.P., Maylie, J., and Sah, P. (2012). Small-conductance Ca<sup>2+</sup>-activated K<sup>+</sup> channels: form and function. *Annu. Rev. Physiol.* 74, 245–269.
- Baudry, M., and Bi, X. (2013). Learning and memory: an emergent property of cell motility. *Neurobiol. Learn. Mem.* 104, 64–72.
- Baudry, M., Kramar, E., Xu, X., Zadran, H., Moreno, S., Lynch, G., Gall, C., and Bi, X. (2012). Ampakines promote spine actin polymerization, long-term potentiation, and learning in a mouse model of Angelman syndrome. *Neurobiol. Dis.* 47, 210–215.
- Benjamin, A.S., and Tullis, J. (2010). What makes distributed practice effective? *Cognit. Psychol.* 61, 228–247.
- Bianchetta, M.J., Lam, T.T., Jones, S.N., and Morabito, M.A. (2011). Cyclin-dependent kinase 5 regulates PSD-95 ubiquitination in neurons. *J. Neurosci.* 31, 12029–12035.
- Bonifacino, J.S., Cosson, P., and Klausner, R.D. (1990). Colocalized transmembrane determinants for ER degradation and subunit assembly explain the intracellular fate of TCR chains. *Cell* 63, 503–513.
- Colgin, L.L., Jia, Y., Sabatier, J.M., and Lynch, G. (2005). Blockade of NMDA receptors enhances spontaneous sharp waves in rat hippocampal slices. *Neurosci. Lett.* 385, 46–51.
- Colledge, M., Snyder, E.M., Crozier, R.A., Soderling, J.A., Jin, Y., Langeberg, L.K., Lu, H., Bear, M.F., and Scott, J.D. (2003). Ubiquitination regulates PSD-95 degradation and AMPA receptor surface expression. *Neuron* 40, 595–607.
- Cook, E.H., Jr., Lindgren, V., Leventhal, B.L., Courchesne, R., Lincoln, A., Shulman, C., Lord, C., and Courchesne, E. (1997). Autism or atypical autism in maternally but not paternally derived proximal 15q duplication. *Am. J. Hum. Genet.* 60, 928–934.
- Deschaux, O., Bizot, J.C., and Goyffon, M. (1997). Apamin improves learning in an object recognition task in rats. *Neurosci. Lett.* 222, 159–162.
- Dudek, S.M., and Bear, M.F. (1993). Bidirectional long-term modification of synaptic effectiveness in the adult and immature hippocampus. *J. Neurosci.* 13, 2910–2918.
- Duhovny, D., Nussinov, R., Wolfson, H.J. (2002). Efficient unbound docking of rigid molecules. In: *Proceedings of the Second Workshop on Algorithms in Bioinformatics (WABI)* (Springer Verlag).
- Ehlers, M.D. (2003). Activity level controls postsynaptic composition and signaling via the ubiquitin-proteasome system. *Nat. Neurosci.* 6, 231–242.
- García-Negredo, G., Soto, D., Llorente, J., Morató, X., Galenkamp, K.M., Gómez-Soler, M., Fernández-Dueñas, V., Watanabe, M., Adelman, J.P., Shigemoto, R., et al. (2014). Coassembly and coupling of SK2 channels and mGlu5 receptors. *J. Neurosci.* 34, 14793–14802.
- Guo, L., and Wang, Y. (2007). Glutamate stimulates glutamate receptor interacting protein 1 degradation by ubiquitin-proteasome system to regulate surface expression of GluR2. *Neuroscience* 145, 100–109.
- Hammond, R.S., Bond, C.T., Strassmaier, T., Ngo-Anh, T.J., Adelman, J.P., Maylie, J., and Stackman, R.W. (2006). Small-conductance Ca<sup>2+</sup>-activated K<sup>+</sup> channel type 2 (SK2) modulates hippocampal learning, memory, and synaptic plasticity. *J. Neurosci.* 26, 1844–1853.
- Huang, L., Kinnucan, E., Wang, G., Beaudenon, S., Howley, P.M., Huibregtse, J.M., and Pavletich, N.P. (1999). Structure of an E6AP-UbcH7 complex: insights into ubiquitination by the E2-E3 enzyme cascade. *Science* 286, 1321–1326.
- Huibregtse, J.M., Scheffner, M., Beaudenon, S., and Howley, P.M. (1995). A family of proteins structurally and functionally related to the E6-AP ubiquitin-protein ligase. *Proc. Natl. Acad. Sci. USA* 92, 2563–2567.
- Jiang, Y.H., Armstrong, D., Albrecht, U., Atkins, C.M., Noebels, J.L., Eichele, G., Sweatt, J.D., and Beaudet, A.L. (1998). Mutation of the Angelman ubiquitin ligase in mice causes increased cytoplasmic p53 and deficits of contextual learning and long-term potentiation. *Neuron* 21, 799–811.
- Jurd, R., Thornton, C., Wang, J., Luong, K., Phamluong, K., Kharazia, V., Gibb, S.L., and Ron, D. (2008). Mind bomb-2 is an E3 ligase that ubiquitinates the N-methyl-D-aspartate receptor NR2B subunit in a phosphorylation-dependent manner. *J. Biol. Chem.* 283, 301–310.
- Kim, J.Y., Kim, M.K., Kang, G.B., Park, C.S., and Eom, S.H. (2008). Crystal structure of the leucine zipper domain of small-conductance Ca<sup>2+</sup>-activated K<sup>+</sup> (SK(Ca)) channel from *Rattus norvegicus*. *Proteins* 70, 568–571.
- Komander, D., Reyes-Turcu, F., Licchesi, J.D., Odenwaelder, P., Wilkinson, K.D., and Barford, D. (2009). Molecular discrimination of structurally equivalent Lys 63-linked and linear polyubiquitin chains. *EMBO Rep.* 10, 466–473.
- Kramár, E.A., Babayan, A.H., Gavin, C.F., Cox, C.D., Jafari, M., Gall, C.M., Rumbaugh, G., and Lynch, G. (2012). Synaptic evidence for the efficacy of spaced learning. *Proc. Natl. Acad. Sci. USA* 109, 5121–5126.
- Kumar, S., Talis, A.L., and Howley, P.M. (1999). Identification of HHR23A as a substrate for E6-associated protein-mediated ubiquitination. *J. Biol. Chem.* 274, 18785–18792.
- Lin, A.W., and Man, H.Y. (2013). Ubiquitination of neurotransmitter receptors and postsynaptic scaffolding proteins. *Neural Plast.* 2013, 432057.
- Lin, M.T., Luján, R., Watanabe, M., Adelman, J.P., and Maylie, J. (2008). SK channel plasticity contributes to LTP at Schaffer collateral-CA1 synapses. *Nat. Neurosci.* 11, 170–177.
- Lin, A., Hou, Q., Jarzylo, L., Amato, S., Gilbert, J., Shang, F., and Man, H.Y. (2011). Nedd4-mediated AMPA receptor ubiquitination regulates receptor turnover and trafficking. *J. Neurochem.* 119, 27–39.
- Lussier, M.P., Nasu-Nishimura, Y., and Roche, K.W. (2011). Activity-dependent ubiquitination of the AMPA receptor subunit GluA2. *J. Neurosci.* 31, 3077–3081.
- Lynch, G., Rex, C.S., Chen, L.Y., and Gall, C.M. (2008). The substrates of memory: defects, treatments, and enhancement. *Eur. J. Pharmacol.* 585, 2–13.
- Lynch, G., Kramár, E.A., Babayan, A.H., Rumbaugh, G., and Gall, C.M. (2013). Differences between synaptic plasticity thresholds result in new timing rules for maximizing long-term potentiation. *Neuropharmacology* 64, 27–36.
- Mabb, A.M., and Ehlers, M.D. (2010). Ubiquitination in postsynaptic function and plasticity. *Annu. Rev. Cell Dev. Biol.* 26, 179–210.
- McKay, B.M., Oh, M.M., Galvez, R., Burgdorf, J., Kroes, R.A., Weiss, C., Adelman, J.P., Moskal, J.R., and Disterhoft, J.F. (2012). Increasing SK2 channel activity impairs associative learning. *J. Neurophysiol.* 108, 863–870.
- Mu, Y., Otsuka, T., Horton, A.C., Scott, D.B., and Ehlers, M.D. (2003). Activity-dependent mRNA splicing controls ER export and synaptic delivery of NMDA receptors. *Neuron* 40, 581–594.
- Ngo-Anh, T.J., Bloodgood, B.L., Lin, M., Sabatini, B.L., Maylie, J., and Adelman, J.P. (2005). SK channels and NMDA receptors form a Ca<sup>2+</sup>-mediated feedback loop in dendritic spines. *Nat. Neurosci.* 8, 642–649.
- Ohtsuki, G., Piochon, C., Adelman, J.P., and Hansel, C. (2012). SK2 channel modulation contributes to compartment-specific dendritic plasticity in cerebellar Purkinje cells. *Neuron* 75, 108–120.
- Patrick, G.N., Bingol, B., Weld, H.A., and Schuman, E.M. (2003). Ubiquitin-mediated proteasome activity is required for agonist-induced endocytosis of GluRs. *Curr. Biol.* 13, 2073–2081.
- Pignatelli, M., Piccinin, S., Molinaro, G., Di Menna, L., Rizzoli, B., Cannella, M., Motolese, M., Vetere, G., Catania, M.V., Battaglia, G., et al. (2014). Changes in mGlu5 receptor-dependent synaptic plasticity and coupling to Homer proteins in the hippocampus of Ube3A hemizygous mice modeling Angelman syndrome. *J. Neurosci.* 34, 4558–4566.

- Qin, Q., Baudry, M., Liao, G., Noniyev, A., Galeano, J., and Bi, X. (2009). A novel function for p53: regulation of growth cone motility through interaction with Rho kinase. *J. Neurosci.* 29, 5183–5192.
- Rapoport, M., and Lorberbaum-Galski, H. (2009). TAT-based drug delivery system—new directions in protein delivery for new hopes? *Expert Opin. Drug Deliv.* 6, 453–463.
- Ren, Y., Barnwell, L.F., Alexander, J.C., Lubin, F.D., Adelman, J.P., Pfaffinger, P.J., Schrader, L.A., and Anderson, A.E. (2006). Regulation of surface localization of the small conductance Ca<sup>2+</sup>-activated potassium channel, Sk2, through direct phosphorylation by cAMP-dependent protein kinase. *J. Biol. Chem.* 281, 11769–11779.
- Roche, K.W., Standley, S., McCallum, J., Dune Ly, C., Ehlers, M.D., and Wenthold, R.J. (2001). Molecular determinants of NMDA receptor internalization. *Nat. Neurosci.* 4, 794–802.
- Schneidman-Duhovny, D., Inbar, Y., Nussinov, R., and Wolfson, H.J. (2005). PatchDock and SymmDock: servers for rigid and symmetric docking. *Nucleic Acids Res.* 33, W363–W367.
- Smith, K.E., Gibson, E.S., and Dell'Acqua, M.L. (2006). cAMP-dependent protein kinase postsynaptic localization regulated by NMDA receptor activation through translocation of an A-kinase anchoring protein scaffold protein. *J. Neurosci.* 26, 2391–2402.
- Stackman, R.W., Hammond, R.S., Linardatos, E., Gerlach, A., Maylie, J., Adelman, J.P., and Tzounopoulos, T. (2002). Small conductance Ca<sup>2+</sup>-activated K<sup>+</sup> channels modulate synaptic plasticity and memory encoding. *J. Neurosci.* 22, 10163–10171.
- Standley, S., Roche, K.W., McCallum, J., Sans, N., and Wenthold, R.J. (2000). PDZ domain suppression of an ER retention signal in NMDA receptor NR1 splice variants. *Neuron* 28, 887–898.
- Sun, J., Liu, Y., Moreno, S., Baudry, M., and Bi, X. (2015). Imbalanced mechanistic target of rapamycin C1 and C2 activity in the cerebellum of Angelman syndrome mice impairs motor function. *J. Neurosci.* 35, 4706–4718.
- van Woerden, G.M., Harris, K.D., Hojati, M.R., Gustin, R.M., Qiu, S., de Avila Freire, R., Jiang, Y.H., Elgersma, Y., and Weeber, E.J. (2007). Rescue of neurological deficits in a mouse model for Angelman syndrome by reduction of alphaCaMKII inhibitory phosphorylation. *Nat. Neurosci.* 10, 280–282.
- Vick, K.A., 4th, Guidi, M., and Stackman, R.W., Jr. (2010). In vivo pharmacological manipulation of small conductance Ca(2+)-activated K(+) channels influences motor behavior, object memory and fear conditioning. *Neuropharmacology* 58, 650–659.
- Wang, Y., Zhu, G., Briz, V., Hsu, Y.T., Bi, X., and Baudry, M. (2014). A molecular brake controls the magnitude of long-term potentiation. *Nat. Commun.* 5, 3051.
- Williams, C.A., Zori, R.T., Stone, J.W., Gray, B.A., Cantu, E.S., and Ostrer, H. (1990). Maternal origin of 15q11-13 deletions in Angelman syndrome suggests a role for genomic imprinting. *Am. J. Med. Genet.* 35, 350–353.
- Xirodimas, D., Saville, M.K., Edling, C., Lane, D.P., and Lain, S. (2001). Different effects of p14ARF on the levels of ubiquitinated p53 and Mdm2 in vivo. *Oncogene* 20, 4972–4983.
- Xu, W., Wong, T.P., Chery, N., Gaertner, T., Wang, Y.T., and Baudry, M. (2007). Calpain-mediated mGlur1alpha truncation: a key step in excitotoxicity. *Neuron* 53, 399–412.
- Yashiro, K., Riday, T.T., Condon, K.H., Roberts, A.C., Bernardo, D.R., Prakash, R., Weinberg, R.J., Ehlers, M.D., and Philpot, B.D. (2009). Ube3a is required for experience-dependent maturation of the neocortex. *Nat. Neurosci.* 12, 777–783.